19th Brazilian Congress of Thermal Sciences and Engineering
November 06th-10th, 2022, Bento Gonçalves - RS - Brazil

ENC-2022-0137
AN EXPERIMENTAL METHOD FOR THE STUDY OF OSCILLATIONS OF PIPES CARRYING LIQUID AND GAS MIXTURES IN SLUG FLOW PATTERN

Sergio N. Bordalo[1]
Celso K. Morooka[2]
Caio C. O. Trigo[3]
State University of Campinas, School of Mechanical Engineering, R. Mendeleyev 200, 13083-860, Campinas, SP, Brazil
[1] bordalo@unicamp.br, [2] morooka@unicamp.br, [3] ctrigo87@unicamp.br

Abstract. *In this paper, the results of an experimental study on a laboratory model of a submersed suspended flexible pipe oscillating due to the internal two-phase slug flow of liquid and gas are presented. The slug flow was produced by injection of sixteen combinations of water and air into the pipe, which was set in catenary configuration inside a water tank with a depth of two meters. The oscillation of the pipe was recorded by cameras registering the position of targeted points on the body of the pipe, providing the time-history of the movement of the pipe. The flow rates of both phases were measured, as well as the speed of the slugs and their frequencies, leading to the evaluation of their lengths and hold-ups, and assessment of the fluid loads applied to the pipe due to gravity and curvature. The amplitudes and frequencies of oscillations of the pipe were obtained processing the video images of the pipe movement. The methodology developed here may be used for numerous geometries and flow states, and it should be useful for validations of numerical simulations of pipe excitation through the comparison between experimental data and computer calculations. The application to offshore pipes in operations, carrying oil and gas from petroleum reservoirs submarine wells to floating facilities in the ocean, may be obtained by the proper scaling up in conjunction with computer simulations.*

Keywords: *offshore, risers, oscillation, slug-flow, experimental*

1. Introduction

Engineering often requires experimental methods to build knowledge, and in this endeavor one faces challenges such as the adequate representation of real scale field operations with small scale laboratory apparatus, and the issue of measurement with satisfactory non-interference. In the present work, an attempt is conducted to study the oscillations of risers, employed in offshore petroleum production, caused by the loads due to the internal two-phase flow of liquid-gas mixtures in slug patterns. Risers are very long and relatively slender pipes connecting floating production units (FPU; platforms or ships) at sea level to the subsea pipelines conducting oil and gas effluents from petroleum wells, under deep and ultra-deep waters. These risers are suspended by one end at the FPU, while part of it lies on the seabed. Therefore, a long stretch of them is somewhat free to move, although limited by the physical constraints at the top and bottom ends. Although made of rigid steel pipes, their length and diameter provide enough flexibility to allow bending. Consequently, under loads caused by sea currents (drag and vortex shedding), movements of the FPU (forced by waves and winds), and the internal fluids (weight and flow momentum), the riser's body may present oscillatory movements and deformation. Field operations occur in depths within typical ranges of thousands of meters (1000m-3000m), which makes real scale experiments very difficult, specially considering the harsh sea states of the marine environment. One alternative, followed here, is to build small scale apparatus, despite inherent disadvantages. Nevertheless, laboratory results may be translated to corresponding real operational conditions with the proper scale transformations or with the help of computer simulations. In the next section, the experimental apparatus will be described. At the same time, the measurement method will be explained. Displacement and deformation is not very difficult under static conditions, but a moving flexible body presents non trivial complications, specially if one does not want to disturb the natural movement of the body. With this objective in mind, video cameras may be used, as done in this work, to track the movement of many target points on the body, frame by frame, as time progresses. In the problem at hand, one crucial information is the excitation load causing the oscillation of the pipe's body. Therefore, one also needs to measure the properties of the internal slug flow, which is an intermittent pattern, with a characteristic speed and periodic spacial mass distribution. Usually, this is done with

internal or external flow probes. In the present experiments, it was possible to use cameras to record the flow through a transparent pipe, and to determine the slug flow main features from the acquired images.

The study of risers transporting two-phase flows is relevant because liquid and gas flow are very common in offshore pipelines and risers during oil and gas production from subsea petroleum reservoirs. Slug flow configurations represent a large fraction of these flows and the intermittency of this type of pattern induces load variation along the flowline, which will prompt oscillations, which may compromise the service lifetime of the riser. Presently, the literature presents a large amount of research regarding the mechanical response behavior of risers when excited by ocean current, waves and platform forced oscillations (Chakrabarti and Frampton, 1982; Mourelle, 1993; Huang et al, 2021). In Figure 1, a typical configuration of an offshore catenary shaped riser pipe for petroleum production is shown (on the left), illustrating the elements from the environment – sea currents, waves, winds, platform motions – which usually excite the system forcing the riser to vibrate.

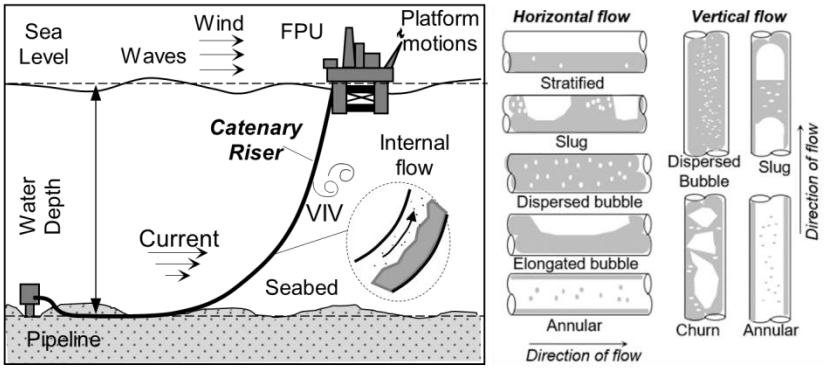

Figure 1. Left: subsea riser carrying the reservoir fluids to the Floating Petroleum Unit (FPU). Right: two-phase flow patterns presented in horizontal and vertical flows of liquids and gases.

In the past, many studies were done on the exciting forces due to each element of the ocean environment, acting isolated from each other or in combination with each other. A lot of work has been done to predict the sea current drag and Vortex Induced Vibration (VIV) effects, as in Morooka et al, 2003 and 2009, Coelho et al, 2005, Kubota et al, 2005, Tsukada, 2016, and, more recently, new procedures have emerged to improve and optimize wave-current interaction effects on risers (Yin et al, 2021). Riser dynamics excited by the internal two-phase flow (Valdivia et al, 2007; Bordalo et al, 2008; Yamamoto, 2010; Ortega et al, 2012; Ma and Srinil, 2018) have received more attention lately, because of their impact on the reduction of riser service life due to oscillations induced stresses on the pipe slender body. In Figure 1 (on the right), two-phase flow patterns are depicted for horizontal and vertical configurations. Some of those patterns exhibit a non-uniform streamwise distribution of mass, typically alternating liquid and gas (e.g., slug flow). In those cases, the intermittent variation of mass crossing a section causes a variation of the flow loads on the pipe's body.

Bordalo et al (2015) fleshed out the influence of the riser loads induced by internal flow of two-phase oil and gas mixtures on the motion of slender risers hanging from floating production units in curved configurations, as used for offshore petroleum production in deep waters. A simulation model to compute non-uniform slugs to provide a tool for the analysis of the dynamic behavior of horizontal pipelines in subsea petroleum production systems has been presented (Santos, 2020). Following up on those theoretical developments, fundamental experiments are needed to validate the mathematical models and the simulation algorithms.

This paper details the experiment conducted with a submersed catenary shaped flexible pipe, suspended inside a water tank, transporting two-phase flows of liquid and gas at various flow rates. The two-phase flows generated at the bottom entrance of the catenary pipe model are modulated to create different slug flow patterns to excite the pipe and induce oscillations. A description is given in the next section of the two-phase flows generated, the procedure to register the riser oscillations, and the determination of the frequencies and amplitudes of motion.

2. Experimental Method

The experiment was conducted in a water tank, in still water. The main test section is a rectangular box measuring 2.1×2.2×0.8 meters. In Figure 2, a sketch is shown of the general overview of the arrangement of the water tank and the pipe model set up. The water tank structure is made of a steel frame with thick glass plates resistant to the water pressure. The photos on the left of Figure 2 show the riser model inside the water tank, with target marks along its length, and the transparent flow visualization window (note the xyz reference).

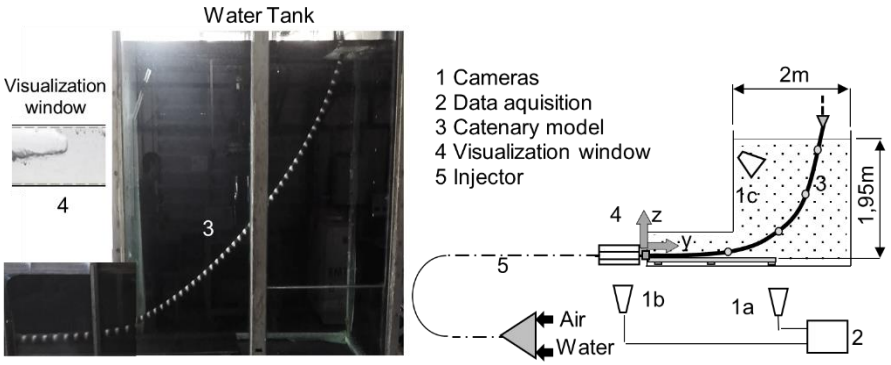

Figure 2. Main elements of the experimental set up: (1a) riser's plane camera; (1b) internal flow camera; (1c) transversal plane camera; (2) data acquisition equipment; (3) suspended flexible catenary pipe model with attached camera targets; (4) transparent pipe for flow visualization; (5) flow mixer and injector.

Two video cameras are positioned, as shown, outside of the water tank. One camera (1a) is in front of the tank's glass plate, facing the yz plane containing the stationary catenary, in order to capture movements of the pipe model. Another camera (1b) is employed to register the motion of the slugs entering the pipe model, recording the flow viewed through a transparent entry pipe (visualization window). Fifty five markers are attached along the pipe length at 50 mm intervals, to be used as targets for the image acquisition system, in order to record their instantaneous position as a function of time. A third camera (1c) is used to monitor movements in the x direction, transversal to the plane of the static catenary. The frame rates are 60 fps, for cameras "1a" and "1c", and 120 fps for camera "1b".

The collected images are stored and later processed with the aid of software with a library of functions that allows the determination of the center of each target in each video frame. This task results in a record file with the x, y and z positions of all the targets during the test runs.

An injector (Figure 2, item 5) was designed and built to generate two-phase flows from a source of pressurized water and a source of compressed air. At the inlet of the injector, regulated nozzles are used to set up the flow rates of each fluid independently, with the aid of flow metering devices.

Throttling the nozzles' valves of the injector, various flow states can be provided at the exit of the injector. The range of flow states is presented in Table 1, in which Q_L and Q_G are, respectively, the volumetric flow rates of liquid and gas (water and air), and A is the flow area of the pipe. Slug flow was obtained for all flow states in this range. The two-phase flow is carried through a very long flow development pipe (10 m) in order to get a stable flow before entering the riser model at the bottom. The flow emerges at the top of the pipe and is collected in a storage tank, from where it is discarded.

Table 1. Two-phase flow states.

Flow Rates	1	2	3	4
Q_L/A (m/s)	0.304	0.516	0.727	0.939
Q_G/A (m/s)	0.238	0.886	1.534	2.282

The pipe model is a synthetic commercial flex-hose (with the properties E and m' shown in Table 2), which is suspended in a catenary configuration with the dimensions given in Table 2. The pipe is held at the top end (Figure 3) by a fixed support joint (hinged to rotate freely with respect to x and y), while, at the bottom, the pipe lays on a hard flat bed, and the bottom end of the pipe is anchored at the flow entry fitting, which connects to the external inlet transparent pipe, where the flow visualization is recorded.

Table 2. Properties of the pipe model.

Parameter	Value	Unit
Riser model length, L_r	2750	mm
External diameter, D	36	mm
Internal diameter, D_i	25	mm
Depth of riser's bed[1], H_{rb}	1950	mm
Top support position[2], H_{top}	150	mm
Horizontal projection[3], Y_{hp}	2600	mm
Touch Down Point[3] (TDP), Y_{tdp}	230	mm
Static vertical supporting force[4], F_{tz}	5.4	N

Static supporting angle[4,5], θ_t	66	degree
Modulus of elasticity, *E*	2.0	MPa
Linear mass of the pipe, *m'*	0.940	kg/m

[1] Below the water level. [2] Above the water level. [3] With respect to the anchor point. [4] At the top support point. [5] With respect to the vertical direction y.

Two frames of a video recorded through the visualization window (Figure 2, item 4) with the camera "1b" (Figure 2) are shown in Figure 3.

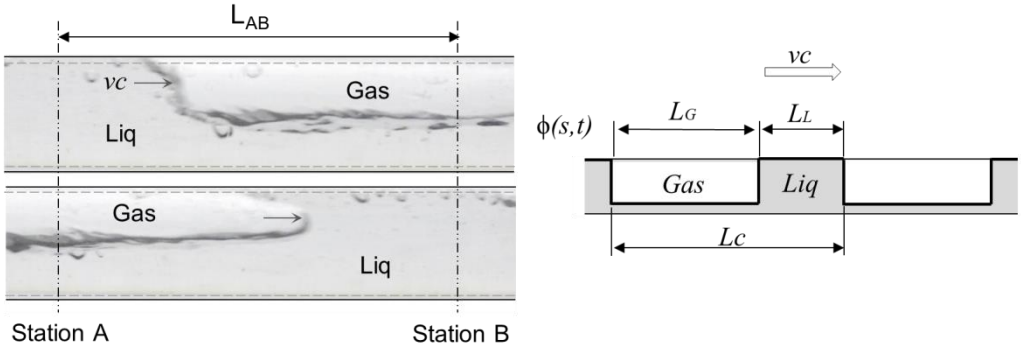

Figure 3. Left: two video frames showing, respectively, the front of a liquid slug and the nose of a gas pack, as they travel between stations A and B. Right: Simplified mass distribution model for the slug flows.

In the top frame (left of Figure 3), the front of the liquid surge can be seen entering, from left to right, the monitored pipe transparent span, just as it crosses "station A". After a while, the liquid slug travels along the length of that pipe span (L_{AB} = 80 mm), crosses "station B" and exits the visualization window, being tailed by a long gas pack. In the bottom frame, the nose of the gas pack can be seen just as it follows the liquid slug, after crossing "station A". The video recordings are processed frame by frame to determine when the liquid slug arrives a "station A" and "station B". The velocity of the slug cell is obtained from

$$v_c = \frac{L_{AB}}{\Delta t_{AB}}\,, \tag{1}$$

in which, L_{AB} is the length of the span between "station A" and "station B", and Δt_{AB} is the time it takes for the slug to travel from one station to the other, obtained from the number of video frames N_{AB} recorded and the frame recording period T_r with

$$\Delta t_{AB} = N_{AB}.T_r\,. \tag{2}$$

The video recordings are also processed to determine each time that every sequential slug arrives at "station A", thus providing the period of passage of the slug cell T_c. Therefore, the slug cell frequency is

$$f_c = \frac{1}{T_c}. \tag{3}$$

The length of the slug cell (and its intermittency $I_c = 1/L_c$), is then calculated from

$$L_c = v_c.T_c\,. \tag{4}$$

In Figure 3, a simplified geometric model of the passing slug cells is illustrated as a mass distribution $\phi(s,t)$ that varies in the streamwise direction "*s*" and with time "*t*", as the slug cells travel along the pipe with velocity v_c; where ϕ is the fraction of liquid filling up a local section of the pipe cross section area of flow A. In the present paper, ϕ is depicted as idealized "square" waves – $\mathbf{w}[(x - v_c.t)/L_c]$ – for the sake of expediency, moving with velocity v_c. The characteristics of the wave **w** are given as follows: The length of the liquid slug, L_L, and of the gas pack (L_G) can be extracted from the video recordings by determining the duration of time it takes for the liquid body to pass through "station A", Δt_L; thus

$$L_L = v_c.\Delta t_L\,, \tag{5}$$

$$L_G = L_c - L_L \, . \tag{6}$$

Due to gravity, there is a somewhat stable film of stratified liquid along the pipe, which flows under the gas pack, and corresponds to a fraction ϕ_f, estimated from (see Figure 4)

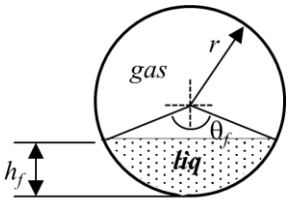

Figure 6. Liquid mass under the gas pack.

$$\phi_f = \left(\theta_f - sin\theta_f\right)/2\,\pi \, , \tag{7}$$

$$\theta_f = 2cos^{-1}\left(1 - \frac{h_f}{r}\right) \tag{8}$$

in which, r is the internal radius of the cross section and h_f is the level of the liquid film, with respect to the bottom center of the cross section, extracted from the video image.

The hold-up of liquid is one of the traditional variables used in the literature for the characterization of two-phase flows. It expresses the average liquid content of the flow as a volume fraction. Here, it corresponds to the hold-up of one slug cell, given by

$$H_L = \frac{L_L + \phi_f . L_G}{L_c} \tag{9}$$

3. Results and Discussions

The results of the video processing to characterize the slug flow are shown in Table 3. Those values are averaged for a large number of cells passing through the visualization window.

Table 3. Characteristics of the slug flow in the model pipe.

Flow State	v_c (m/s)	f_c (Hz)	L_c (m)	ϕ_f	L_L (m)	L_G (m)	H_L	*Flow State*	v_c (m/s)	f_c (Hz)	L_c (m)	ϕ_f	L_L (m)	L_G (m)	H_L
{1,1}	2.39	0.59	4.05	0.24	3.21	0.84	0.50	**{2,1}**	2.87	1.08	2.66	0.25	0.69	1.97	0.83
{1,2}	3.73	0.67	5.57	0.24	4.87	0.70	0.44	**{2,2}**	2.78	1.00	2.78	0.25	2.23	0.55	0.49
{1,3}	4.50	0.63	7.14	0.24	6.41	0.73	0.43	**{2,3}**	4.58	0.87	5.26	0.24	4.39	0.87	0.46
{1,4}	5.89	0.59	9.99	0.25	8.96	1.03	0.43	**{2,4}**	5.66	0.84	6.74	0.25	5.87	0.87	0.44
{3,1}	3.14	1.61	1.95	0.25	1.33	0.62	0.55	**{4,1}**	5.50	2.03	2.71	0.25	1.76	0.95	0.56
{3,2}	4.44	1.26	3.52	0.25	2.63	0.89	0.51	**{4,2}**	5.86	2.05	2.86	0.25	2.04	0.82	0.52
{3,3}	3.92	1.28	3.06	0.26	2.38	0.68	0.48	**{4,3}**	5.69	1.84	3.09	0.25	2.35	0.74	0.48
{3,4}	6.38	1.53	4.17	0.25	3.30	0.87	0.48	**{4,4}**	7.63	1.83	4.17	0.22	3.29	0.88	0.38

Reading key – Flow State: **{i,j}** corresponds to the flow rate pair Q_{Gi} and Q_{Lj}.

Figure 5.a depicts the slug frequencies superimposed on the flow state map. It should be noticed that the flow intermittency leads to a range of frequencies, and it is well known that the frequency of excitation is one of the paramount factors to affect the amplitude of the oscillations of a body. Roughly, for each liquid flow rate, the frequency increases with the gas flow rate. The effect of the liquid flow rate is less pronounced, in this range of flow states. Figures 5.b and 5.c map the slugs' speed and hold-up.

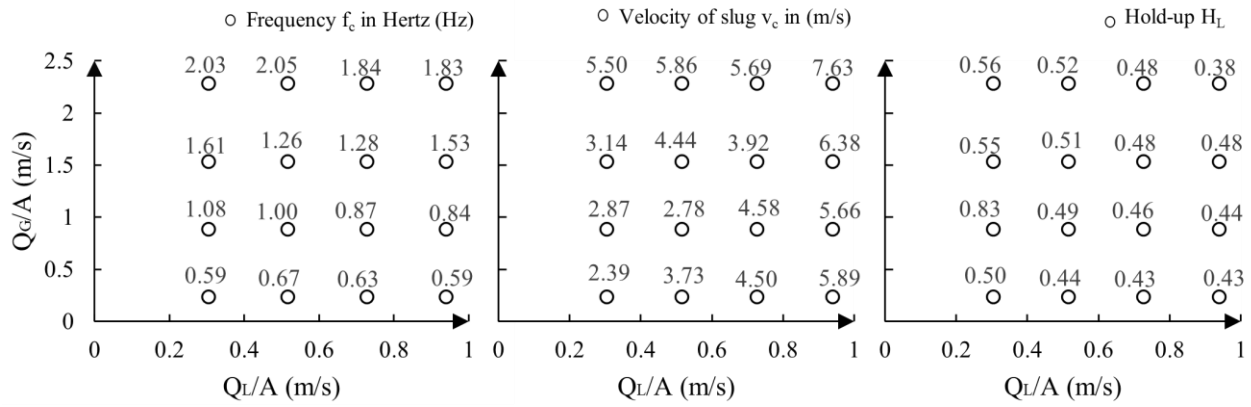

Figure 5. Flow states: (a) slug frequencies; (b) slug speeds; (c) cell's hold-ups.

In Figure 6 below, one example of processing the slug tracking in the visualization window is depicted. The raw signal from the image pixels extracted from the videos is draw on the top graph of Figure 6, showing the non-dimensional gas-liquid interface (h/D_i), obtained by pixel shade contrast. The bottom graph displays the square wave model (previously presented in Figure 3) of the moving mass distribution of the flow after fitted to the data. The evaluation of the frequency f_c is obtained from the averaged periods, for several slug cells passing along the window.

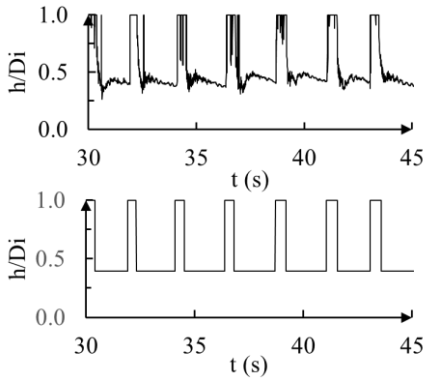

Figure 6. Slug signal processing: top - raw camera signal, bottom – square wave fitted to the signal.

In Figure 7, the results of displacements of the targets on the pipe's body (both, vertical direction *z*, and horizontal direction *y*), obtained from the video camera recording, are shown plotted along the pipe length for each time frame, during 4 s, as an example. A displacement is defined here as the difference between the target position coordinate at any time and its initial static position. The blank strips in this graphs are due to the supporting struts that hold the glass panels of the water tank, and blind the camera filming the riser model (these structural elements are seen in the photo of the apparatus in Figure 2).

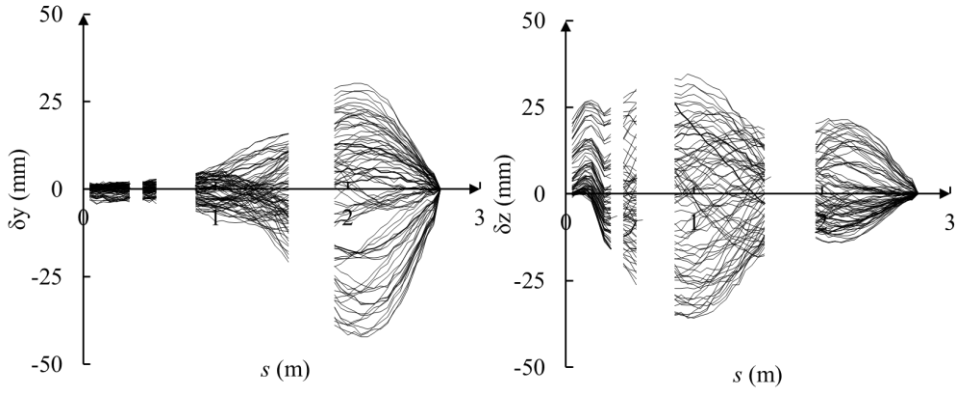

Figure 7. Displacements in the horizontal, *y*, and vertical, *z*, directions for 4 s.

Among the fifty five points monitored along the length of the model pipe, sample points A, B, C and D were selected to be used as examples here. The chosen points are shown in Figure 8. An example of the local tangent (**T**) and normal (**N**) directions of the pipe body shape (in the yz plane) at each selected point is drawn for point B in this figure. These local frames of reference are defined by the inclination (α) of **T** with respect to the global horizontal direction, and are useful when describing local variables. The coordinates of the highlighted points and the inclination (α) of the pipe at those points are given in Table 4 below.

Table 5. Coordinates of samples points (y,z) and tangent inclination (a).

Points	y (mm)	z (mm)	α (°)	Points	y (mm)	z (mm)	α (°)
A	510	40	9	C	2030	920	49
B	1400	375	33	D	2460	1590	69

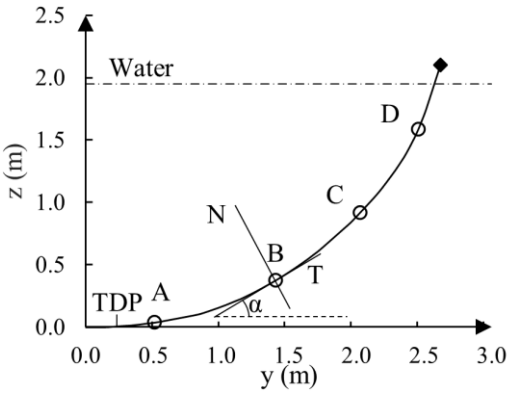

Figure 8. Samples points along the length of the pipe model (coordinates and inclinations on Table 5).

Sixteen flow states were generated as input to the pipe model. The oscillations resulted from flow state {4,3} – Q_{L4}/A = 0.939 m/s and Q_{G3}/A = 1.534 m/s – are presented here. The slug flow pattern, for this flow state, presents an intermittency with a frequency f_{c43} of 1.84 Hz. The oscillations in y and z, at each observation point, are shown in Figure 9.

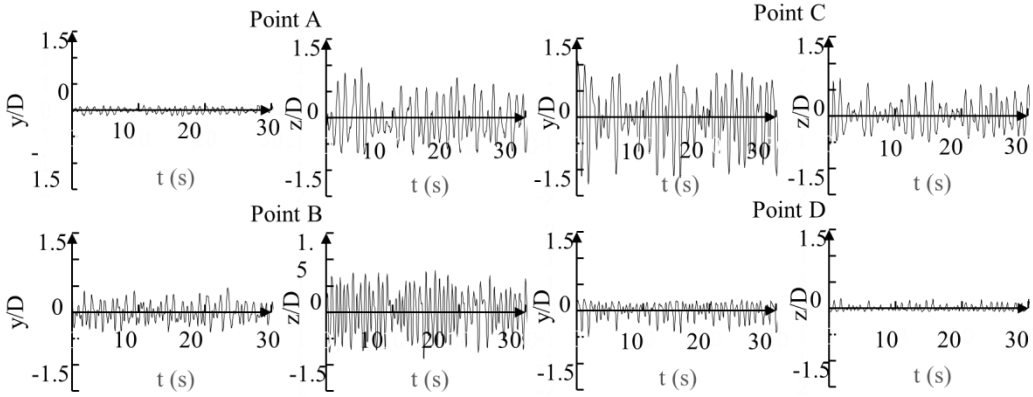

Figure 9. Oscillations at points A, B, C and D in response to the slugs flowing inside the pipe.

The trajectory of each selected point in the yz plane is shown in Figure 10. Those are obtained from the data presented in Figure 9. An ellipsoidal envelope is superimposed to contain the path of the points and, from it, the amplitude A_{major} along the major axis and amplitude A_{minor} along the minor axis of the ellipse are evaluated, as well as the inclination (β) of the major axis of the ellipse with respect to the horizontal direction y. In Figure 11, the major (A_{major}) and minor (A_{minor}) amplitudes, and the inclination β and are plotted along the length of the pipe.

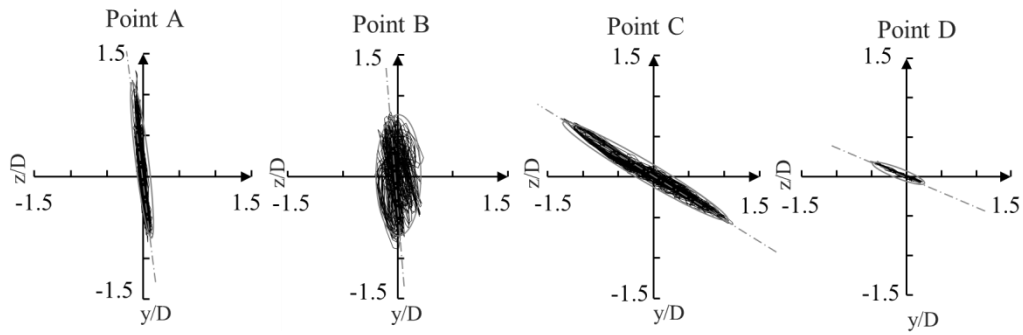

Figure 10. Trajectories of points A, B, C and D on the yz plane enclosed by ellipsoidal envelopes, also showing the inclination β of the major axis with respect to the horizontal direction y.

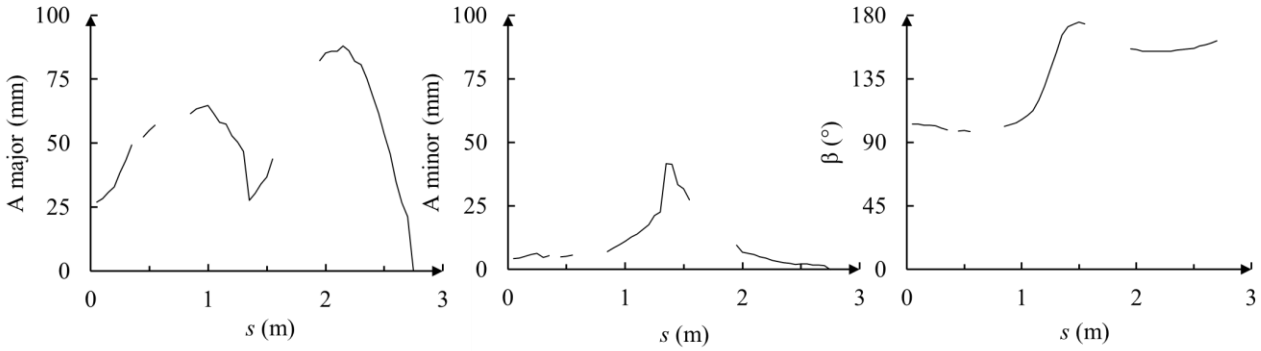

Figure 11. (left) The major amplitude, $A_{major\ ;}$ (center) the minor amplitude A_{minor} , (right) the inclination β.

In Figure 12, the amplitudes along the major and minor axis of the trajectories of each point of observation are shown versus the frequency f_c of the imposed slugs. The inclination β is also shown in Figure 12.

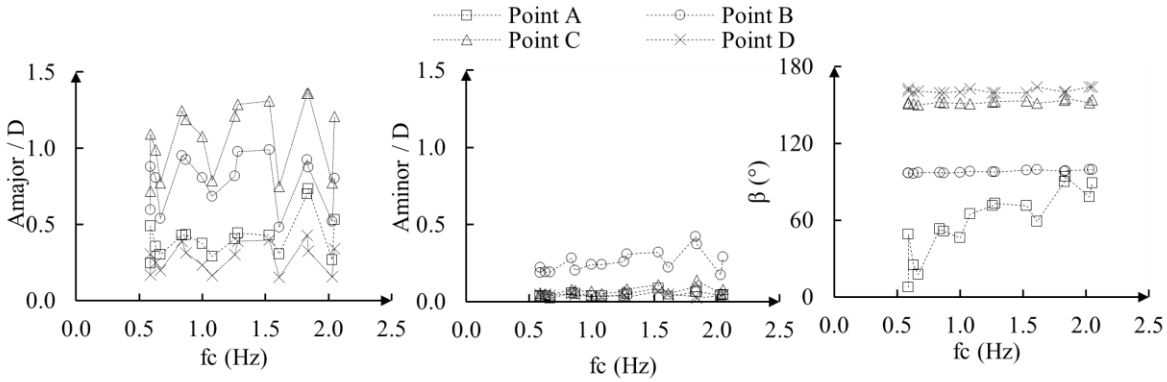

Figure 12. Amplitudes along the major axis (left) and minor axis (center) of the trajectories of each point of observation, and the inclination of the major axis β of the envelopes of the trajectories of the selected points (right).

The movement of each point (shown in Figures 9 and 10) is affected by its location along the pipe's body. Points closer to the ends are influenced by the boundary conditions imposed by the type of constrain at that end. At the top end, the pipe extremity is hanging from a pinned type of support, therefore the stretch of pipe on the top may be able to swing (similarly to a hanging pendulum). Of course, cannot swing freely because of the rest of the pipe body below it. On the other end, at the bottom, the extremity is fixed at the inlet flow fitting anchoring the pipe, which restrains that end to behave similarly to a horizontal cantilever end, and forces the pipe's body to bend in order to move (generating bending stresses). For the catenary shape, a significant length of pipe lays on the floor due to its weight, between the anchor point and the touchdown point (TDP – where the pipe starts to ascend to the surface). Consequently, the suspended body near to the TDP bends and its points move up and down. Regarding the "principal" direction of movement (indicated by the

major axis of the envelope), in general, it is pretty close to the direction normal (**N**) to the body static configuration. The **N** direction, with respect to the horizontal, is describe by the angle β_o given by

$$\beta_o = \alpha + 90° \tag{10}$$

The average angle β for the trajectories of points A, C and D (respectively 98°, 152° and 161°) are near β_o (respectively, 99°, 139° and 159°). Likely because those points suffer greater constraints due to the boundary conditions. It is observed that, for these points, β does not change very much for different flow rates and slug frequencies. Which indicates a strong limitation induced by the geometry, as discussed before. On the other hand, point B is freer to wander around in the yz plane. Its envelope is actually broader that the envelopes of A, C and D, which are somewhat svelter (Figure 10).

In Figure 13, the frequency of the pipe oscillation f_s is plotted against the frequency of the slug cells f_c, which are the only origin for the imposed intermittent loads on the pipe's body. There seems to be, as expected, some correlation between cause and effect. However, this seems to be non-trivial. An explanation for this result requires further exploratory research. At this time, from visual inspection of the time history recorded, it seems that the oscillation of the pipe presents frequencies in ranges close to the frequency of the slugs, but also other frequencies emerge. A study of the frequency spectrum should be conducted in order to shed light on how the pipe and the slugs interact.

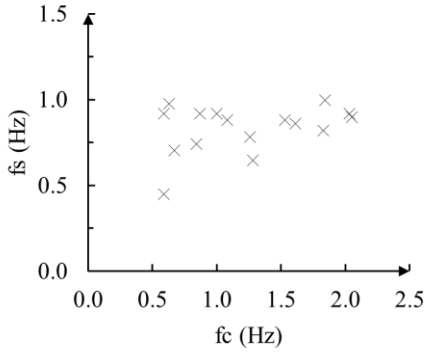

Figure 13. Frequencies of the oscillations against the frequency of the slugs.

Further analysis is required to advance the understanding of the dynamics of the observed oscillations with respect to the excitation. Mainly, regarding the frequency of the slugs and the frequencies of the response of the pipe, displayed in Figure 13. The effects of the magnitude of the gravity and curvature loads applied to the body of the flexible pipe also need to be deeply studied, in order to provide answers to the questions that arise from the observation of Figures 9 to 12. A simple reasoning, that does not take into account all the dynamic effects present in these oscillations, might not pass a rigorous scrutiny. A computer 3D time-simulation based on the laws of dynamics is needed to analyze the movement of the pipe, as presented by Bordalo and Morooka, 2018.

4. Conclusions

This paper deals with the development of an experimental method to obtain data about oscillations and its forcing cause, in the case of suspended pipes carrying mixtures of liquid and gas, which is an important issue in offshore petroleum production. With regard to the case sample presented in this paper, it was successfully shown that the internal flow may excite a flexible catenary pipe with significant displacements (magnitudes greater than one diameter) even when no other external effects are present (such as currents, waves, movements of the supporting rig). The observed excitation is caused by intermittency of the flow mass distribution which causes intermittent gravity forces and intermittent curvature induced forces along the length of the pipe. It was demonstrated that the oscillations depend on the flow state of the slugs.

Through the present work we've concluded that the experimental method developed and tested here with video cameras is adequate and presents interesting advantages to provide important data to help in the investigation of the oscillation of risers driven by slug flows. First, one important advantage of the present method is non-interference; i.e., there are no measurement devices attached to the body or interacting with it causing added inertia or external forces that would affect the dynamics. Second, another aspect of this methodology is its flexibility and range of application. It may be used for many other configurations of pipes and risers, and for various flow rates of interest for the operations in the industry. Third, this procedure provides various pieces of information from the recordings; such as coordinates, velocities, frequencies and periods, amplitudes, and pipe shapes as functions of time. The results obtained with this method may be used in the advancement of calculation algorithms to design subsea pipelines and risers or to monitor the ones in operation. These are engineering problems of great concern because oscillations induce variable stresses which have a negative

effect on the duration of the useful lifetime of the pipes. The output of simulators can be validated against the recorded movements of the model under controlled conditions as shown here.

A number of improvements can be added with more expensive instruments and laboratory investments, such as: cameras of higher resolution, higher speed, and more cameras per length of pipe, flow meters for broader ranges and higher resolution, larger storage volume for digital data, custom designed flexible pipe to configure the mechanical properties, larger water tank for larger scale experiments, to name a few. Experiments could also be extended to vary the properties of the catenary (diameter, length, depth, weight, elasticity etc); to vary the mixing liquid and gas (densities, viscosities), to vary the range of two-phase flows (flow rates and patterns), to study other configuration of the pipe – lazy-wave, steep-wave, vertical, horizontal free-span, jumpers etc. Future experiments could include composed effects like internal slug flow and external water current or imposed movement at the support joint end. The regular mass distribution model for the slugs f(s,t) employed in the present work can be refined in a number of ways as mentioned by Bordalo and Morooka, 2018.

5. Acknowledgements

The authors would like to acknowledge the continuing support of the Coordenação de Aperfeiçoamento de Pessoal de Nível Superior (CAPES) and the São Paulo Research Foundation (FAPESP). The second author would like also to thank the Brazilian National Council for Scientific and Technological Development – CNPq. Acknowledgments are extended to the National Petroleum Agency (ANP).

6. References

Bordalo, S.N.; Morooka, C.K.; Cavalcante, C.C.P.; Matt, C.G.C.; Franciss, R.: Whipping Phenomenon Caused by the Internal Flow Momentum on the Catenary Risers of Offshore Petroleum Fields, ASME 27th International Conference on Offshore Mechanics and Arctic Engineering, Estoril, Portugal 2008.

Bordalo, S.N.; Morooka, C.K.; Oliveira, A.P.: Modeling the Forces Induced by the Two-Phase Flow on Deep Water Production Risers, SPE Artificial Lift Conference - Latin America and Caribbean, Salvador-Bahia, Brazil, 2015.

Bordalo, S.N.; Morooka, C.K.: Slug flow induced oscillations on subsea petroleum pipelines. Journal of Petroleum Science and Engineering, v. 165, p. 535-549, 2018.

Chakrabarti, S.K. and Frampton, R.E.: Review of Riser Analysis Techniques, Applied Ocean Research, Vol. 4, No. 2, 1982

Coelho, F.M.; Shiguemoto, D.A.; Morooka, C.K.: Description of a Vertical Riser Behavior in Frequency and Time Domain, 18th International Congress of Mechanical Engineering - COBEM, Ouro Preto-MG, 2005.

Huang, W.; Wu, X.; Liu, J.; Bai, X.: Dynamics of Deepwater Riser: Theory and Method, Springer; 1st ed., ISBN-10: 9811628874; ISBN-13: 978-9811628870, 2022.

Kubota, H.Y.; Suzuki, H.; Morooka, C.K.: Evaluation of a Top Tensioned Riser Model for Experiments, 18th International Congress of Mechanical Engineering - COBEM, Ouro Preto-MG, 2005.

Ma, B.; Srinil, N.: Dynamic Characteristics of Deep-Water Risers Carrying Multiphase Flows, ASME 37th International Conference on Ocean, Offshore and Arctic Engineering (OMAE), Madrid, Spain, 2018.

Morooka, C.K.; Kubota, H.Y.; Nishimoto, K.; Ferrari Jr., J.A.; Ribeiro, E.J.B.: Dynamic Behavior of a Vertical Production Riser by Quasi 3D Calculations, ASME 22th International Offshore Mechanics and Arctic Engineering (OMAE) Conference, Cancún, 2003.

Morooka, C.K.; Tsukada, R.I.; Silva, S.; Franciss, R.; Matt, C.G.C.: Model Test of a Steel Catenary Riser in a TowingTank, ASME 28th International Conference on Ocean, Offshore and Arctic Engineering, Honolulu. USA, 2009.

Mourelle, M.M.: Dynamic Analysis of Structural Systems Composed of Risers and Anchor Lines. Ph.D. thesis, Federal University of Rio de Janeiro, December, Rio de Janeiro, Brazil, 1993.

Ortega, A.; Rivera, A.; Nydal, O. J.; Larsen, C. M.: On the Dynamic Response of Flexible Risers Caused by Internal Slug Flow, 31st International Conference on Ocean, Offshore and Arctic Engineering, Rio de Janeiro, Brazil, 2012.

Santos, G.M.; Bordalo, S.N.; Morooka, C.K.: Modeling Dynamic Loads Induced by Slug Flows Considering Gas Expansion due to the Pressure Gradient in a Horizontal Hanging Pipeline, SPE Annual Technical Conference and Exhibition (ATCE), Virtual Conference, 2020.

Tsukada, R.I. and Morooka, C.K.: A Numerical Procedure to Calculate the VIV Response of a Catenary Riser, Ocean Engineering, v. 122, p. 145-161, 2016.

Valdivia, P.G.; Frizzone, C.M.R.; Matt, C.G.C.; Franciss, R.: Experimental Verification of the Whipping Phenomenon on Offshore Catenary Risers Caused by the Internal Flow Momentum, 19th International Congress of Mechanical Engineering - COBEM, Brasília, 2007.

Yamamoto, M.; Murai, M.: A Numerical Analysis of the Internal Flow Effect on the Riser's Mechanical Behavior, ASME 2010 29th International Conference on Ocean, Offshore and Arctic Engineering, Shanghai, China, 2010.

Yin et al: Optimization of Hydrodnamic Coefficients for VIV Prediction, ASME 40th International Conference on Ocean, Offshore and Arctic Engineering, Virtual Online, 2021.

7. Responsibility notice

The authors are the only responsible for the printed material included in this paper.